Over 100 mW Stable Low-Noise Single-Frequency Ring-Cavity Fiber Laser Based on a Saturable Absorber of Bi/Er/Yb co-doped Silica Fiber

Ying Wan, Jianxiang Wen, Chen Jiang, Kai Zou, Fengzai Tang, Fufei Pang, and Tingyun Wang

***Abstract*—Two kinds of Yb-doped fibers were fabricated, namely, Yb: YAG crystal-derived silica fibers (YCDSFs) with a gain coefficient of 6.0 dB/cm, and Bi/Er/Yb co-doped silica fibers having a Yb concentration of 0.13×10^{26} ions/m^3. Based on these fibers, a ring-cavity single-frequency fiber laser (SFFL) has been constructed, in which the YCDSF was used as a gain medium and the Bi/Er/Yb co-doped fiber acted as a saturable absorber. It has been demonstrated that the SFFL had an over 100 mW output at 1030 nm, a slope-efficiency of up to 18.3%, and an optical signal-to-noise ratio of over 63 dB. The fluctuation of the output power of the laser was less than 0.65% of 103.5 mW within 10 hrs and no mode-hopping was observed for 5 hrs. The SFFL had a linewidth <7.5 kHz at the maximum output power, and the measured relative intensity noise was lower than −142 dB/Hz at the frequency above 1.0 MHz. The results indicate that the ring-cavity SFFL built could be used as a laser source for applications in high-power fiber laser and high-precision optical fiber sensing and detection.**

***Index Terms*—Bi/Er/Yb co-doped fiber, Ring-cavity, Single-frequency, Yb: YAG crystal-derived silica fiber**

I. INTRODUCTION

Single-frequency fiber lasers (SFFLs) can be used as laser sources for a wide variety of applications, such as high-precision optical fiber sensing, seeding of high-power fiber lasers, Internet of Things, and laser radars [1-3]. Particularly, the SFFLs based on the Yb-doped fibers for the ~1.0 μm wavelength operation are highly demanded for uses in seed sources for high-power fiber laser and high-power boosters for gravitational wave detection [4]. To meet the increasingly potential applications, the performance of ~1.0 μm SFFLs, i.e., linewidth, maximum output power, and stability, needs to be further improved. These parameters are the key indicators determining the resolution, sensitivity and stability of the system used for optical detection, sensing, and imaging [5-7]. Various cavity schemes have been proposed to generate single-longitudinal-mode (SLM) operation, typically, a distributed Bragg reflector (DBR) [8, 9], a distributed feedback (DFB) configuration [10] and a long linear cavity [11, 12], as well as a traveling-wave ring cavity [13-15]. Each of them has its associated advantages and drawbacks. For instance, the ultrashort cavity configuration of DBR and DFB can allow them to achieve a SLM operation at high output powers, but, the significant heat accumulated in ultrashort gain fibers may cause laser instability such as sharp increase in linewidth [8, 9]. In contrast, the approaches of long linear cavity and traveling-wave ring cavity can render sufficient heat dissipation, narrow theoretical linewidth, and low noise. This makes them a powerful means that can be used to develop stable ultra-narrow (<10 kHz) linewidth SFFLs [16, 17]. However, the long linear cavity SFFLs are prone to spatial hole burning (SHB) effect, resulting in instability and the occurrence of mode-hopping.

In addition to above designs, the ring cavity structure has also been accomplished [13-15]. It can effectively avoid the SHB effect, and also provide the system flexibility and wavelength tunability. Despite these merits, the long cavity length in SFFLs may cause multi-longitudinal-mode (MLM) oscillation, deleterious to laser performance. To mitigate this, a number of ultra-narrowband filters have been introduced in the ring cavity laser, such as Fabry-Perot cavity-based filters [13], sub-ring resonators based on cursor effect [14], and ultra-narrowband induced grating with a saturable absorber (SA) based on two-dimensional materials and unpumped Yb-doped fibers [15, 18, 19]. Among them, the SFFLs with a section of unpumped Yb-doped fiber can not only offer an all-fiber structure but also a low insertion loss. In the meantime, the bandwidth of the induced grating can be purposely tailored through the design of doped fiber, such as dopant concentration, relative refractive index profile, and absorption and emission cross-sections [20, 21]. Therefore, the use of unpumped gain fiber-based filter renders a high degree of flexibility for the system to obtain a SLM output.

Manuscript received XXX XX, 2021; revised XXX XX, 2021; accepted XXX XX, 2021. This work was supported by National Key Research and Development Projects (2020YFB1805800), Natural Science Foundation of China (61975113, 61935002, 61675125, 61635006), 111 Project (D20031), and Shanghai professional technical public service platform of advanced optical waveguide intelligent manufacturing and testing (19DZ2294000). (*Corresponding author: Jianxiang Wen.*)

Y Wan, J Wen, J Chen, K Zou, F Pang, and T Wang are with the Key Lab of Specialty Fiber Optics and Optical Access Networks, Joint International Research Laboratory of Specialty Fiber Optics and Advanced Communication, School of Communication and Information Engineering, Shanghai University, 99 Shangda Road, Shanghai 200444, China (e-mail: yingwan@shu.edu.cn; wenjx@shu.edu.cn; jiangchen17@shu.edu.cn; zoukai@shu.edu.cn; ffpang@shu.edu.cn; tywang@shu.edu.cn).

F Tang is with the WMG, University of Warwick, Coventry, CV4 7AL, UK (fengzai.tang@warwick.ac.uk).

Color versions of one or more figures in this article are available at http://ieeexplore. ieee.org.

Digital Object Identifier 10.1109/JLT.2021.xxxxxxx

This article has been accepted for publication in a future issue of this journal, but has not been fully edited. Content may change prior to final publication. Citation information: DOI 10.1109/JLT.2021.3124227, Journal of Lightwave Technology

On the other hand, however, the performance of such SFFLs needs to be improved on the level of output powers, slope efficiency, and the stabilities in output powers and longitudinal mode operation [19, 22-24]. The effective approach is deemed to be optimization of the gain fiber and the unpumped Yb-doped fiber. The use of high-gain active fiber can enhance the laser output powers [24, 25]. For the selection of gain fiber, Yb: YAG crystal-derived silica fiber (YCDSF) could be an ideal candidate in terms of its high concentration doping, high gain coefficient, and inherent compatibility with commercial silica fibers [8, 26]. For instance, Gao et al. in 2020 obtained the SLM operation using a ring-cavity laser based on only 10-cm-long YCDSF, whose output power was as high as 45 mW, although the gain coefficient of the YCDSF was low [24]. In addition, in order to achieve narrow bandwidth of induced grating, conversely, low concentration Yb-doped fibers are required for the SA fibers. In this regard, most commercial Yb-doped fibers cannot meet such as a demand [14, 19, 22-24], and could result in poor stability of the SFFLs.

In this work, a ring-cavity fiber laser with the incorporation of two home-made Yb-doped fibers has been demonstrated, in which the YCDSF and the Bi/Er/Yb co-doped fiber were used as a gain medium and a SA respectively. The stable SLM operation of the laser has been accomplished, and the lasing characteristics have also been systematically evaluated, including its slope efficiency, longitudinal mode and power stability, noise, and so on.

II. Yb-Doped Silica Fibers And Ring-Cavity SFFL Construction

(1) Yb: YAG crystal-derived silica fiber

High-concentration YCDSFs were made using a 15 at.% Yb: YAG single crystal rod and a high-purity silica substrate tube. At 2050 °C, the fibers were drawn on a CO_2 laser-heated drawing tower using the melt-in-tube method. The detailed fabrication process was reported in our previously work [27].

The elemental distribution along the diameter of the YCDSF was characterized using an electron probe micro-analyzer (EPMA-1720, SHIMADZU, Japan). As shown in Fig. 1(a), the mutation of element content is observed at the boundary between the cladding and core layer. The elements of Si, Yb, Y, and Al concentrations in the core layer were 25.96, 6.57, 18.21, and 8.49 wt.%, respectively.

The background loss of the YCDSF was measured using a cut-back method, in which a 1550 nm single wavelength laser acted as the light source. In Fig. 1(b), the fitted slope shows a background loss of 0.6 dB/m.

The unsaturated absorption characteristic was used to describe the optical pumping efficiency of the YCDSF. The absorption coefficient as a function of pump power at 980 nm is presented in Fig. 1(c), revealing the saturated and unsaturated absorption coefficients (α_s and α_{us}) of 26.49 and 0.88 dB/cm respectively. The subsequently calculated merit factor of the unsaturated absorption (M_a) is 96.8%, suggesting that the YCDSF can be efficiently pumped by the 980 nm laser.

The measured gain coefficient of the YCDSF is shown in Fig. 1(d) for three different signal light powers of -25, -5, and 5 dBm

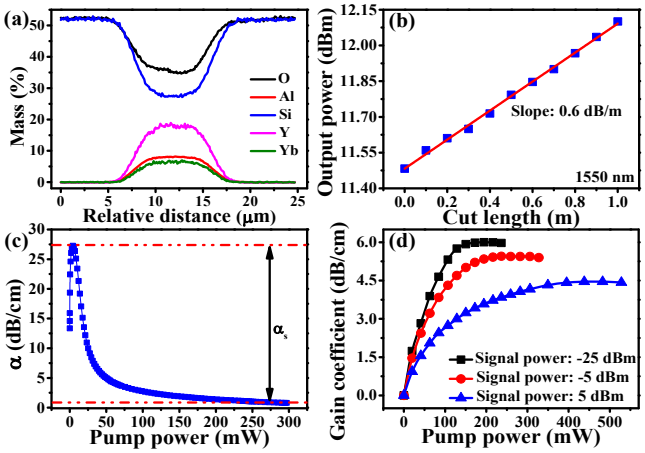

Fig. 1. (a) Elemental distribution curve along the diameter of the fiber. (b) The background loss of the YCDSF at 1550 nm. (c) The unsaturated absorption of YCDSF at 980 nm. (d) The gain coefficient at different signal powers as a function of pump power.

as a function of the 980 nm pump power. In each signal case, the gain coefficient gradually increases with the increased pump light power, before reaching its saturation. The pump power required to achieve gain saturation is also increased with increasing the signal light power from -20, -5, to 5 dBm, whereas the corresponding saturation gain coefficients drops from 6.0, 5.5, to 4.1 dB/cm respectively. The maximum gain coefficient of the YCDSF is 6.0 dB/cm.

(2) Bi/Er/Yb co-doped silica fiber

Bi/Er/Yb co-doped silica fibers were fabricated using a modified chemical vapor deposition (MCVD) process combining with the atomic layer deposition (ALD) technique (TFS-200, Beneq Inc., Finland) on a graphite-heated drawing tower. The detailed fabrication process has been reported in Ref. [28]. The cross-sectional view of the fiber is shown as the inset in Fig. 2(a). The core and cladding diameters of the fiber are 9.2 and 125.1 μm, respectively. According to the EPMA test result, the doping concentrations of Yb and Er ions in the fiber core are 0.012 and 0.014 wt.% respectively, and the number of ions per unit volume of Yb is about 0.13×10^{26} ions/m^3. The refractive index distribution of the fiber was measured using a refractive index profiler (S14, Photon Kinetics, Inc., U.S.). The refractive index difference (Δn) between the fiber core and cladding was approximately 0.0050, and the refractive index of the fiber core layer is 1.4606 (Fig. 2(a)). The effective mode refractive index is 1.4594 at 1030 nm.

The absorption spectrum of the fiber was measured using a broadband source (BBS, SC-5, YSL Photonics, China) and an optical spectrum analyzer (OSA, AQ6370, YOKOGAWA, Japan). The result is depicted as the inset in Fig. 2(b), where four absorption peaks can be seen. Two absorption peaks of electronic transitions of Er ions are observed at 800 ($^4I_{15/2}\rightarrow{}^4I_{9/2}$) and 1530 nm ($^4I_{15/2}\rightarrow{}^4I_{13/2}$). The absorption peaks at 918 and 978 nm were mainly originated from the $^2F_{7/2}\rightarrow{}^2F_{5/2}$ transition of Yb ions. Based on the obtained absorption spectrum of the Yb ion, the absorption cross sections (σ_{abs}) can be calculated by the equation as below [29]:

$$\sigma_{abs}(\lambda) = \frac{2.303}{NL} OD(\lambda) \quad (1)$$

This article has been accepted for publication in a future issue of this journal, but has not been fully edited. Content may change prior to final publication. Citation information: DOI 10.1109/JLT.2021.3124227, Journal of Lightwave Technology

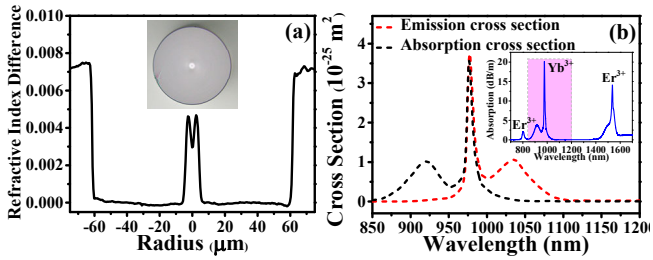

Fig. 2. The refractive index distribution (a) and the absorption and emission cross sections (b) of Bi/Er/Yb co-doped silica fiber.

where OD(λ) is the optical density obtained by the absorption spectrum, N is the number of ions per unit volume of the Yb ion, and L is the length of the test fiber. The emission cross sections (σ_{em}) of the fiber can be evaluated using the McCumber theory [29]:

$$\sigma_{em}(\lambda) = \sigma_{abs}(\lambda) exp\left[\frac{(\varepsilon - h\nu)}{KT}\right] \quad (2)$$

where ε is the energy of zero-phonon-line, h is the Planck constant, ν is the working frequency, K is the Boltzmann constant, and T is the temperature in Kelvin, which is 300 K in this case. The results are depicted in Fig. 2(b). The σ_{abs} and σ_{em} of Bi/Er/Yb co-doped silica fiber are 7.4×10^{-27} m^2 and 1.15×10^{-25} m^2 at 1030 nm. These values are lower than those of the commercial Yb-doped fibers [23, 24], which mainly depend on low Yb doping concentration. At the same time, the introduction of Bi and Er ions may further reduce the emission cross-section of Yb ions by the energy transfer process from Yb ions to Er ions and bismuth active centers.

(3) Ring-cavity SFFL setup

A backward pump scheme was applied in setting up the ring-cavity SFFL (Fig. 3), namely, a single mode 980/1030 nm wavelength division multiplexer (WDM) to input the pump light at 980 nm and output the amplified spontaneous emission (ASE) of YCDSF simultaneously. The cross-sectional and side views of the YCDSF are depicted in Figs. 3(a) and (b). The ASE light can be transmitted along the optical circulator (CIR) and the SA fiber, and reflected back by the fiber Bragg grating (FBG), forming a ring resonant cavity. The FBG has a reflectivity of 70.0%, corresponding to a 3 dB bandwidth of 0.05 nm. As shown in Figs. 3(c)→(d), the FBG was utilized not only as the wavelength selective device but also as the laser output port. The 1030 nm laser can generate a standing wave through light interference of two counter propagating waves in the SA fiber. The periodic change of refractive index occurs along the SA fiber, from which a transient-induced grating (also called standing-wave FBG) can be generated. A Bi/Er/Yb co-doped silica fiber is used as the SA fiber, whose period of the induced grating (Λ) is about 352.9 nm. The standing wave FBG has a typical ultra-narrow bandwidth of tens of MHz, which can further narrow the bandwidth of the laser to achieve a SLM output. The process is schematically illustrated in Figs. 3(d)→(e)→(f). A compact polarization controller (PC) was deployed to control the polarization state within the laser cavity, ensuring a stable SLM operation.

According to the setup, the longitudinal mode spacing (Δν) of fiber laser can be evaluated using equation (3)

$$\Delta\nu = \frac{c}{nl} \quad (3)$$

where c is the speed of light, n is the fiber refractive index, and l is the cavity length of the laser.

The reflection bandwidth (Δυ) of the laser depends on the bandwidth of the transient self-induced grating formed by the SA. Based on the Kramers-Kronig relation [30], refractive index changes periodically along the SA fiber due to the different absorbance of light at nodes and antinodes. The bandwidth of induced grating can be written as equation (4)

$$\Delta\upsilon = \frac{c}{2\pi n_{eff} L_g}\sqrt{(\kappa L_g)^2 + \pi^2} \quad (4)$$

where L_g and n_{eff} are the length of induced grating and effective index of SA fiber respectively; κ is coupling coefficient, which can be expressed as equation (5)

$$\kappa = \frac{\pi\delta n_{max}}{\lambda} \quad (5)$$

where λ is the work wavelength of laser; δn_{max} is the maximum refractive index change in Bi/Er/Yb co-doped silica fiber, which can be given by equation (6)

$$\delta n_{max} \sim \frac{\Gamma_s N \lambda \sigma_{em}}{4\pi} \quad (6)$$

where Γ_s, N, and σ_{em} are overlapping factor, Yb ions dopant concentration and emission cross-section at the working wavelength, respectively.

To obtain the SLM operation, the relationship between Δν and Δυ, equation (7), needs to be satisfied:

$$\Delta\upsilon \le 2\Delta\nu \quad (7)$$

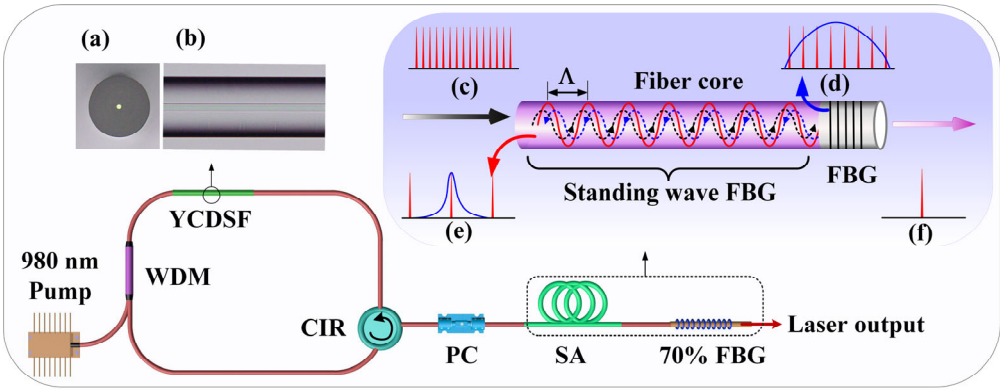

Fig. 3. Setup of ring-cavity SFFL based on YCDSF and Bi/Er/Yb co-doped silica fibers.

This article has been accepted for publication in a future issue of this journal, but has not been fully edited. Content may change prior to final publication. Citation information: DOI 10.1109/JLT.2021.3124227, Journal of Lightwave Technology

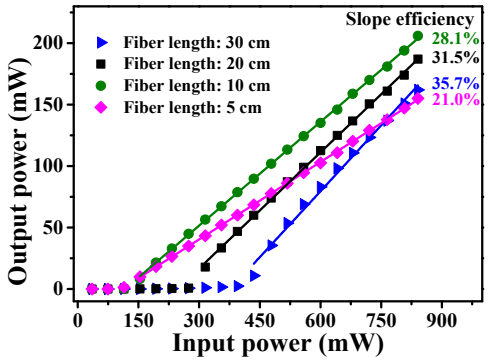

Fig. 4. Output power of the fiber laser as a function of pump power across different YCDSF lengths at the condition without using the SA fiber.

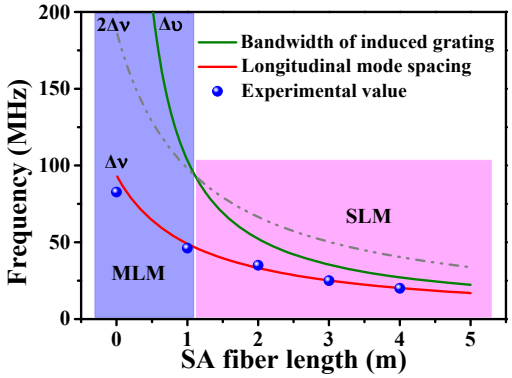

Fig. 5. Calculated longitudinal mode spacing and the bandwidth of induced grating as a function of the SA fiber length.

According to Equations (3)-(7), a larger longitudinal mode spacing and a narrower induced grating bandwidth would facilitate the laser SLM operation. However, the longitudinal mode spacing is inversely proportional to the laser cavity length, and the induced grating bandwidth is proportional to the SA fiber length. Therefore, each component of the laser cavity needs to be carefully designed.

First, to optimize the length of the YCDSF, the ring-cavity lasers with different YCDSF lengths, i.e., 5, 10, 20, and 30-cm, were tested in the absence of SA fiber according to the relationship between the pump power and laser output power. Figure 4 shows the results. It can be found that both the threshold power and slope efficiency of the laser increases, as the length of the YCDSF increases. Due to the limitation of pump power, however, the maximum output power of laser does not increase with increasing the YCDSF length. At the 10 cm YCDSF length, the maximum output power, slope efficiency, and threshold power are up to 206 mW, 28.1%, and as low as 140 mW, respectively, showing an overall better performance over others. Consequently, the 10-cm-long YCDSF was chosen as the gain fiber, and the total cavity length of the laser system without the SA fiber is 2.2 m.

In order to obtain SLM operation, the length of the SA fiber is also evaluated. For Bi/Er/Yb co-doped silica fiber, the typical parameters used are Γ_s =0.7, σ_{em} =0.115 × 10^{-24} m^2, N=0.13×10^{26} ions/m^3, and λ=1030 nm. As shown by the red curve in Fig. 5, the value of Δν falls as the SA fiber becomes longer. According to Equation (6), δn_{max} is 0.85×10^{-7}. The

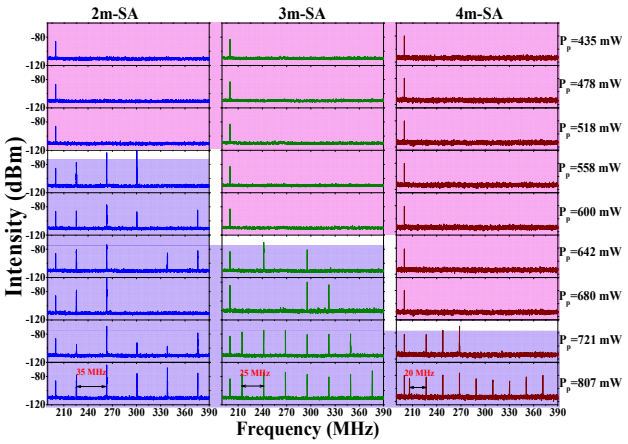

Fig. 6. Radio frequency beating spectra of the fiber laser with the 2, 3, and 4 m SA fiber at different pump powers.

bandwidth of the induced grating as a function of the SA fiber length is estimated using Equations (4) and (5), as shown by the green curve in Fig. 5. According to the operating conditions of SLM (Equation (7)), the critical fiber length of SA is about 1.13 m, above which the laser operates in a SLM, as designated by the pink rectangular area in the Fig. 5. Otherwise, the laser would operate at the MLM state in the purple rectangular area.

III. Evaluation Of The Single-Frequency Ring-Cavity Fiber Laser

In the light of the above analysis, three ring cavity fiber lasers were built using 2, 3, and 4 m Bi/Er/Yb co-doped silica fibers, respectively. The longitudinal mode characteristics of the fiber lasers were assessed based on the Mach-Zehnder interference, in which a 200 MHz acoustic optical modulator (AOM) was used to generate frequency shift, and the applied electrical spectrum analyzer (ESA, Agilent) had a resolution bandwidth of 2 kHz. Figure 6 presents the measured radio frequency (RF) beating spectra of the fiber lasers at different pump powers. The detection frequency range spanned from 190 to 390 MHz, covering a width of 200 MHz. At each given SA, when the pump power increased, a RF signal skipping was observed from one beating peak to multiple beating peaks, indicative of the change of the laser operating state. The identified skipping pump powers at the SA fiber length of 2, 3, and 4 m are 518, 600, and 680 mW, respectively. In the case with the pump power lower than the skipping pump power, the RF beating spectra show only a prominent beating peak at 200 MHz, indicating that a stable SLM operation has been obtained in the laser, as the pink area marked in Fig. 6. Otherwise, the multiple beating peaks can be observed, suggesting a MLM operation, as the highlighted purple area in Fig. 6. The underlying mechanism may be attributed as follows. As the pump power rises, the signal light power in the SA fiber also is increased. The gradually stronger signal light may pump the SA fiber, and then generate new ASE. These may also result in the slightly refractive index change of the SA fiber, thereby perturbing the bandwidth and stability of the induced grating [20]. Therefore, it is difficult to effectively suppress the mode competition, as also reported in Ref. [25]. At the same time, we also found that the fiber laser with 4 m SA fiber has the largest skipping pump

This article has been accepted for publication in a future issue of this journal, but has not been fully edited. Content may change prior to final publication. Citation information: DOI 10.1109/JLT.2021.3124227, Journal of Lightwave Technology

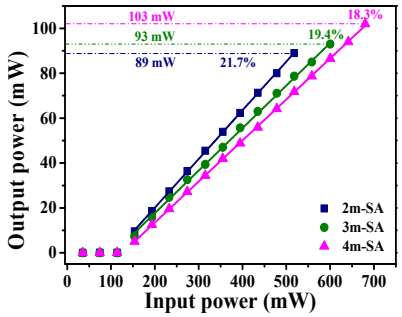

Fig. 7. Output power of the SFFLs as a function of pump power at different SA fiber lengths.

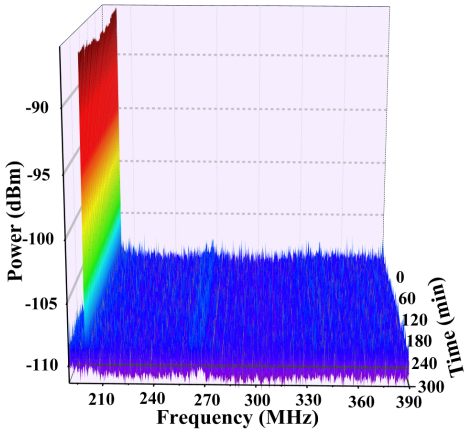

Fig. 8. Radio frequency beating spectra mapping of the laser with 4 m SA fiber at SLM operation within 300 mins.

power, presumably due to the absorption cross section of the SA fiber at 1030 nm is relatively weak. As the length of SA fiber increases, the narrow-band induced grating formed in the fiber becomes more stable, which might be a potential option to suppress mode competition [20].

In addition, at the pump power of 807 mW, the interval of beating signals, namely the longitudinal mode interval, were estimated to be approximately 35, 25, and 20 MHz, corresponding to the laser cavity with the 2, 3, and 4 m SA fibers respectively. These values are consistent with the theoretical calculations, as shown by the blue dot and red curve in Fig. 5.

Under the SLM operation, the output power of the laser was further analyzed as a function of the pump power. As shown in Fig. 7, the output power of the laser increases approximately linearly with increasing the pump power, after passing the lasing threshold. The slope efficiency of the laser decreases from 21.7% to 18.3%, when the SA fiber length increases from 2 to 4 m. This is mainly due to the larger insertion losses of the longer fiber. Since the laser with the 4 m SA fiber shows the largest output power, approximately 103.5 mW, it consequently becomes the focus of the following study in laser performance.

To characterize the longitudinal mode stability of the laser with the 4 m SA fiber at 103.5 mW, the beating signal of the laser was continuously monitored for every 9 s over 300 mins using an ESA with the sweep time of 764 ms. The result (Fig. 8) displays a prominent beating peak at 200 MHz only, manifesting that a mode-hopping-free SLM was obtained in the

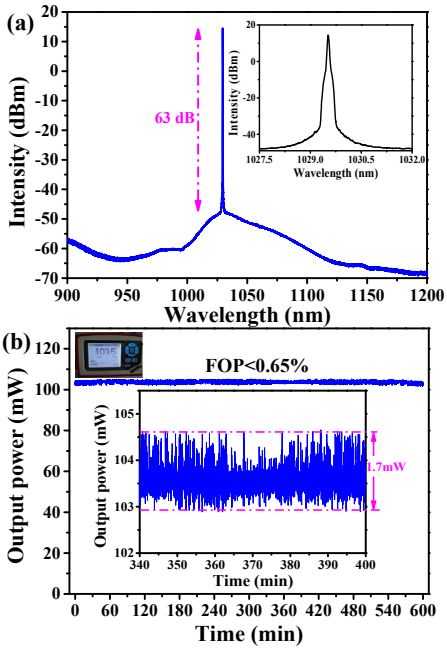

Fig. 9. Output spectrum (a) and power stability (b) recorded within 10 hours of the SFFL with the 4 m SA fiber at the maximum output power.

ring cavity SFFL. The faint line at 265 MHz is presumably caused by the electrical noise. Since the long-term longitudinal mode stability mainly depends on the nature of induced grating, the sufficiently long silica fiber co-doped with a low Bi/Er/Yb concentration used in this work can account for the observed ultra-narrow bandwidth and high stability of the induced grating. Consequently, the system constructed has effectively suppressed the mode competition and the mode change caused by ambient environment.

At the output power of 103.5 mW, the output spectra of the 4 m SA fiber SFFL ranging from 900 to 1200 nm were scrutinized using an OSA with the resolution of 0.02 nm. In Fig. 9(a), an optical signal-to-noise ratio (OSNR) of about 63 dB lasing peak and a typical ASE spectrum of Yb ions [31] with a nearly 120 nm bandwidth were observed. The discernible intensity at the 900-980 nm in the figure can be accounted for by the residual ASE of YCDSF. The magnified region of 1027.5 to 1032.0 nm (inset in Fig. 9(a)) presents a highly symmetrical lasing peak centered at 1029.6 nm, from which an ultra-narrow bandwidth of 0.04 nm at 3 dB can be derived. Compared with the output spectra of the DBR SFFLs [8, 9], the ASE of Yb ions is significantly enhanced because of the structure of laser cavity.

Figure 9(b) shows the power stability of the SFFL with the 4-m SA fiber at 103.5 mW. It was measured using a power meter (PM, Thorlabs), every 1 s for 10 hrs. The fluctuation of the output power (FOP) takes up less than 0.65% (rms) of the average power, and in range from 340 to 400 mins the power variations are <1.7 mW as inset in Fig. 9(b). It is likely that the power fluctuation of the pump laser and the change of the ambient temperature are the main reasons leading to the observed weak instability in output power. In general, the obtained results indicate that the SFFLs have a stable output

This article has been accepted for publication in a future issue of this journal, but has not been fully edited. Content may change prior to final publication. Citation information: DOI 10.1109/JLT.2021.3124227, Journal of Lightwave Technology

TABLE 1
SUMMARY OF THE RING CAVITY SFFLS BASED ON DIFFERENT GAIN FIBERS AND SAS

Gain media		SA fibers		Maximum output power (mW)	Slope efficiency	OSNR (dB)	Power stability	Linewidth (delay line)	RIN (dB/Hz)	Refs.
Yb doped fibers	Fiber length (cm)	Yb doped fibers	Fiber length (m)							
INO Yb 501	50	INO Yb 501	5	6	2.93%	45	<2% within 1 h	760 Hz (30 km)	-92	[22]
Nufern, SM-YSF-HI	150	Nufern, SM-YSF-HI	2	7	/	65	<1.5% within 30 min	<500 Hz (/)	/	[23]
Double-cladding, Nufern PM-YDF-5/130-VIII	250	Nufern, PM-YSF-HI-HP	10	35	21.0%	34	/	<6.0 kHz (11 km)	-134	[19]
YCDSF (4.8 wt.%)	10	Nufern, PM-YSF-HI-HP	2	45	10.2%	60	0.36% within 30 min	<4.3 kHz (48 km)	/	[24]
YCDSF (6.57 wt.%)	10	Bi/Er/Yb co-doped fiber	4	103	18.3%	63	0.65% within 10 h	<7.5 kHz (25 km)	-142	This work

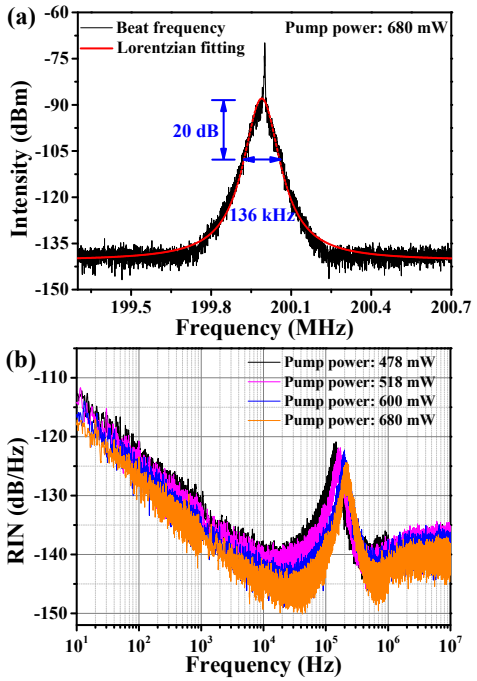

Fig. 10. The heterodyne signal (a) and relative intensity noise (RIN) (b) of the SFFL.

power without the presence of photodarkening effect in YCDSF, and it would be suitable for a seeding of high-power fiber lasers.

The SFFL linewidth was investigated using the delayed self-heterodyne method with a 25-km-long single-mode fiber delay. This delay-line provided a 1.21 ms delay and a 7.5 kHz linewidth resolution. To avoid the interference of low frequency signals, a 200 MHz AOM was introduced. At the maximum output power, a typical heterodyne signal was observed using an ESA with a sweep time of 0.69 s and a 30 Hz bandwidth resolution. In Fig. 10(a), the fitted Lorentzian profile reveals a 20 dB linewidth at 136 kHz on which the laser linewidth can be estimated as about 6.8 kHz. Since the value is less than the linewidth resolution of measurement, it is thus that the laser linewidth should be less than 7.5 kHz.

Figure 10(b) depicts the results of relative intensity noise (RIN) of the SFFL pumped at different powers. In the frequency range of 10 Hz -10 MHz, the RIN spectrum at a given pump power presents a dominant sharp peak at the relaxation oscillation frequency, after which the RIN level off at about -142 dB/Hz. The central frequency of the peak shifts towards higher frequencies as the pump power increases, i.e., from 140.8 kHz at 478 mW to 223.1 kHz at 680 mW, whereas the peak intensity drops from -121.4 dB/Hz to -124.5 dB/Hz correspondingly. No obviously large noise peak was observed. Compared with the ring-cavity SFFLs incorporated with other Yb-doped fibers [22-24], the noise level of this laser is significantly reduced, which can be attributed to the better performances of the YCDSF and Bi/Er/Yb co-doped silica fibers.

Table 1 shows the summary of characteristics of the ring-cavity SFFLs based on different gain fibers and SA fibers. The notable feature of the ring-cavity SFFLs is that the linewidth is very narrow, less than 7.5 kHz [22-24]. It is also seen that the SFFLs based on the commercial high-concentration Yb-doped silica fibers [23, 24] have the lower output powers and slope efficiencies than the one constructed in this work, although they have used the longer gain fibers. This is mainly due to the lower gain coefficient associated with the commercial Yb-doped fibers. As reported in Ref. [19], the cladding pumping scheme can improve the slope efficiency of the laser, but the output power and OSNR still need to be further optimized. Although the introduction of YCDSF may shorten the length of the gain fiber, a significant improvement on the output power and slope efficiency of the SFFL have not been observed in Ref. [24]. Overall, the ring-cavity SFFL incorporated with the home-made YCDSFs and Bi/Er/Yb co-doped fibers in this work has shown a promising improvement in the laser performance, especially in output power, slope efficiency and RIN. It may be drawn upon the following reasons:

(1) A high gain YCDSF is used in the laser system. The gain coefficient of 6 dB/cm in this work is much higher than that of other Yb-doped fibers [19, 22-24].
(2) The applied Bi/Er/Yb co-doped silica fibers enable the

relatively narrow bandwidth of the induced grating. The value of 25 MHz is about half of that of other commercial Yb-doped fiber-based gratings (>50 MHz) [19, 23, 24]. The realization is largely determined by the relatively low Yb-ion doping concentration (0.012 wt.%) and the smaller emission cross-section at 1030 nm, approximately 1.15×10^{-25} m^2 (as shown in Fig. 2(b)). Commercial Yb-doped fibers used for SAs have been reported to be 0.32×10^{26} ions/m^3 in Refs. [19, 24]. Further, the energy transfer of co-doped ions from Yb ions to Er ions and bismuth active centers [32], may also play a role, leading to the reduced emission cross-section of Yb ions.

(3) The combined use of high-gain YCDSF and low-concentration Bi/Er/Yb co-doped silica fiber in the SFFL provides an effective approach to design the laser cavity structure, i.e., two Yb-doped fiber length options and avoid the heat accumulation in the YCDSF but generate the stable ultra-narrowband induced grating at the same time, leading to a low-noise stable SLM output.

As a consequence, it is the unique properties of these two optical fibers that make the SFFL laser to have a high-power, high-efficiency, and low-noise stable laser output. The work presented here provides an alternative method to improve performance of the ring-cavity SFFLs, and could also shed light on the study of other ring cavity SFFLs at different operating wavelengths.

IV. Conclusion

In summary, we have fabricated two kinds of Yb-doped fibers to meet the requirements of high-performance ring-cavity SFFLs, namely, a 10-cm-long YCDSF with a gain coefficient of 6 dB/cm to act as the gain medium, and a 4-m-long Bi/Er/Yb co-doped silica fiber for SA to form a 25 MHz ultra-narrow induced grating. A stable SLM operation has been obtained within the ring-cavity SFFL. The performances of the ring cavity SFFL were significantly improved through optimizing the properties of doped fibers and the configurations of the laser cavity. The maximum output power and slope efficiency of SFFL were up to 103.5 mW and 18.3%, respectively. At the maximum output power, the fiber laser had the OSNR of 63 dB and the linewidth of less than 7.5 kHz. The laser also demonstrated a long-term stability, i.e., FOP < 0.65% of 103.5 mW within 10 hrs and no observation of mode-hopping for 5 hrs. Moreover, its RIN reached around -142 dB/Hz at the frequencies of over 1.0 MHz, and the relaxation oscillation frequency was less than 250 kHz. The study suggests that the high-performance ring-cavity SFFL could be used as a seed/light source in high-power fiber laser and in gravitational wave detection.

References

[1] L. Rodriguez-Cobo, R. A Perez-Herrera, M. A Quintela, R. Ruiz-Lombera, M. Lopez-Amo, and J. M Lopez-Higuera, "Virtual FBGs using saturable absorbers for sensing with fiber lasers," *Sensors*, vol. 18, no. 11, pp. 3593, Oct. 2018.

[2] N. Kuse, T. Tetsumoto, G. Navickaite, M. Geiselmann, and M. E. Fermann, "Continuous scanning of a dissipative Kerr-microresonator soliton comb for broadband, high-resolution spectroscopy," *Opt. Lett.*, vol. 45, no. 4, pp. 927-930, Feb. 2020.

[3] S. C. Kumar, G. K. Samanta, and M. Ebrahim-Zadeh, "High-power, single-frequency, continuous-wave second-harmonic-generation of ytterbium fiber laser in PPKTP and MgO: sPPLT," *Opt. Express*, vol. 17, no. 16, pp. 13711-13726, Jul. 2009.

[4] F. Wellmann, M. Steinke, P. Wessels, N. Bode, F. Meylahn, B. Willke, L. Overmeyer, J. Neumann, and D. Kracht, "Performance study of a high-power single-frequency fiber amplifier architecture for gravitational wave detectors," *Appl. Opt.*, vol. 59, pp. 7945-7950, Sep. 2020.

[5] C. Dixneuf, G. Guiraud, Y. V. Bardin, Q. Rosa, M. Goeppner, A. Hilico, C. Pierre, J. Boullet, N. Traynor, and G. Santarelli, "Ultra-low intensity noise, all fiber 365 W linearly polarized single frequency laser at 1064 nm," *Opt. Express*, vol. 28, no. 8, pp. 10960-10969, Mar. 2020.

[6] F. Wellmann, M. Steinke, F. Meylahn, N. Bode, B. Willke, L. Overmeyer, J. Neumann, and D. Kracht, "High power, single-frequency, monolithic fiber amplifier for the next generation of gravitational wave detectors," *Opt. Express*, vol. 27, no. 20, pp. 28523-28533, Sep. 2019.

[7] T. Wu, X. Peng, W. Gong, Y. Z. Zhan, Z. S. Lin, B. Luo, and H. Guo, "Observation and optimization of ^{4}He atomic polarization spectroscopy," *Opt. Lett.*, vol. 38, no. 6, pp. 986-988, Mar. 2013.

[8] Y. Wan, J. X. Wen, C. Jiang, F. Z. Tang, J. Wen, S. J. Huang, F. F. Pang, and T. Y. Wang, "Over 255 mW single-frequency fiber laser with high slope efficiency and power stability based on an ultrashort Yb-doped crystal-derived silica fiber," *Photon. Res.*, vol. 9, no. 5, pp. 649-656, May. 2021.

[9] Z. J. Liu, Y. Y. Xie, Z. H. Cong, Z. G. Zhao, Z. X. Jia, C. Z. Li, G. S. Qin, S. Wang, X. B. Gao, X. B. Shao, and X. Y. Zhang, "110 mW single frequency Yb: YAG crystal-derived silica fiber laser at 1064 nm," *Opt. Lett.*, vol. 44, no. 17, pp. 4307-4310, Sep. 2019.

[10] O. V. Butov, A. A. Rybaltovsky, A. P. Bazakutsa, K. M. Golant, M. Y. Vyatkin, S. M. Popov, and Y. K. Chamorovskiy, "1030 nm Yb^{3+} distributed feedback short cavity silica-based fiber laser," *J. Opt. Soc. Am. B*, vol. 34, no. 3, pp. A43-A48, Mar. 2017.

[11] M. Yin, S. Huang, B. Lu, H. Chen, Z. Ren, and J. T. Bai, "Slope efficiency over 30% single-frequency ytterbium-doped fiber laser based on Sagnac loop mirror filter," *Appl. Opt.*, vol. 27, no. 27, pp. 6799-6803, Sep. 2013.

[12] R. Poozesh, Kh. Madanipour, and P. Parvin, "Single-frequency gain-switched ytterbium-doped fiber laser at 1017 nm based on dynamic self-induced grating in a saturable absorber," *Opt. Lett.*, vol. 44, no. 1, pp. 122-125, Jan. 2019.

[13] D. Chen, H. Fu, and W. Liu, "Single-longitudinal-mode erbium-doped fiber laser based on a fiber Bragg grating Fabry-Perot filter," *Laser Phys.*, vol. 17, pp. 1246-1248, Sep. 2007.

[14] K. L. Wang, B. L. Lu, Z. R. Wen, X. Y. Qi, J. Y. Ding, H. W. Chen, and J. T. Bai, "Widely tunable ytterbium-doped single-frequency all-fiber laser," *Opt. Laser Technol.*, vol. 128, pp. 106242, Mar. 2020.

[15] T. C. Yin, Y. F. Song, X. G. Jiang, F. H. Chen, and S. L. He, "400 mW narrow linewidth single-frequency fiber ring cavity laser in 2 um waveband," *Opt. Express*, vol. 27, no. 11, pp. 15794-15799, May 2019.

[16] F. Biraben and K. Vahala, "On the high power limit of the laser linewidth," *IEEE J. Quantum Electron.*, vol. 6, no. 6, pp. 889-890, Jun. 1983.

[17] S. A. Havstad, B. Fischer, A. E. Willner and M. G. Wickham, "Loop-mirror filters based on saturable-gain or -absorber gratings," *Opt. Lett.*, vol. 21, no. 21, pp. 1466-1468, Nov. 1999.

[18] Z. H. Sun, X. T. Jiang, Q. Wen, W. J. Li, and H. Zhang, "Single frequency fiber laser based on an ultrathin metal-organic framework," *J. Mater. Chem. C.*, vol. 7, pp. 4662-4666, Feb. 2019.

[19] R. Poozesh, K. Madanipour, and P. Parvin, "High SNR watt-level single frequency Yb-doped fiber laser based on a saturable absorber filter in a cladding-pumped ring cavity," *J. Lightwave Technol.*, vol. 20, no. 20, pp. 4880-4886, Aug. 2018.

[20] S. Stepanov, A. A. Fotiadi, and P. Mégret, "Effective recording of dynamic phase gratings in Yb-doped fibers with saturable absorption at 1064 nm," *Opt. Express*, vol. 15, no. 14, pp. 8832-8837, Jun. 2007.

[21] S. Stepanov, "Dynamic population gratings in rare-earth-doped optical fibres," *J. Phys. D: Appl. Phys.*, vol. 41, pp. 224002, Oct. 2008.

[22] J. Kang, B. L Lu, X. Y. Qi, X. Q. Feng, H. W. Chen, M. Jiang, Y. Wang, P. Fu, and J. T. Bai, "An efficient single-frequency Yb-doped all-fiber MOPA laser at 1064.3 nm," *Chinese Phys. Lett.*, vol. 33, no. 12, pp. 124202, Jul. 2016.

[23] J. W. Chen, Y. Zhao, Y. N. Zhu, S. Liu, and Y. Ju, "Narrow line-width ytterbium-doped fiber ring laser based on saturated absorber," *IEEE Photon. Technol. Lett.*, vol. 29, no. 5, pp. 439-441, Jan. 2017.

[24] X. B. Gao, Z. H. Cong, Z. G. Zhao, G. S. Qin, Z. X. Jia, Y. Y. Xie, M. Y. Jiang, X. Y. Zhang, Z. J. Liu, "Single-frequency kHz-linewidth 1070 nm laser based on Yb: YAG derived silica fiber," *IEEE Photon. Technol. Lett.* Vol. 32, no. 14, pp. 895-898, Jun. 2020.

[25] X. He, S. H. Xu, C. Li, C. S. Yang, Q. Yang, S. P. Mo, D. D. Chen, and Z. M. Yang, "1.95 μm kHz-linewidth single-frequency fiber laser using self-developed heavily Tm^{3+}-doped germanate glass fiber," *Opt. Express*, vol. 21, no. 18, pp. 20800-20805, Aug. 2013.

[26] Y. M. Zhang, G. Q. Qian, X. S. Xiao, X. L. Tian, Z. Chen, J. P. Zhong, Z. J. Ma, and J. R. Qiu, "A yttrium aluminosilicate glass fiber with graded refractive index fabricated by melt-in-tube method," *J. Am. Ceram. Soc.*, vol. 101, pp. 1616-1622, Oct. 2018.

[27] Y. Wan, J. X. Wen, Y. H. Dong, C. Jiang, M. Jia, F. Z. Tang, N. Chen, Z. W. Zhao, S. J. Huang, F. F. Pang, and T. Y. Wang, "Exceeding 50% slope efficiency DBR fiber laser based on a Yb-doped crystal-derived silica fiber with high gain per unit length," *Opt. Express*, vol. 28, no.16, pp. 23771-23783, Aug. 2020.

[28] J. X. Wen, Y. Wan, Y. H. Dong, H. H. Zhang, Y. H. Luo, F. Z. Tang, G. D. West, F. F. Pang, G. D. Peng, and T. Y. Wang, "Spectroscopy of Pb/Bi co-doped silica optical fibers fabricated via atom layer deposition with modified chemical vapour deposition," *J. Lumin.*, vol. 231, pp. 117768, Oct. 2021.

[29] Y. G. Feng, G. Toci, A. Pirri, B. Patrizi, Z. W. Hu, J. B. Wei, H. M. Pan, X. Zhang, X. Y. Li, S. Su, M. Vannini, and J. Li, "Fabrication, microstructure, and optical properties of Yb: $Y_3ScAl_4O_{12}$ transparent ceramics with different doping levels", *J. Am. Ceram. Soc.*, vol. 103, pp. 224-234, Jul. 2020.

[30] V. Lucarini, J. J. Saarinen, K.-E. Peiponen, and E. M. Vartiainen, Kramers-Kronig relations in optical materials research. New York, NY, USA: Springer, 2005, vol. 110.

[31] S. P. Zheng, J. Li, C. L. Yu, Q. L. Zhou, L. L. Hu, and D. P. Chen, "Preparation and characterizations of Yb: YAG-derived silica fibers drawn by on-line feeding molten core approach," *Ceram. Int.*, vol. 43, pp. 5837-5841, Jan. 2017.

[32] Z. M. Sathi, J. Z. Zhang, Y. H. Luo, J. Canning, and G. D. Peng, "Improving broadband emission within Bi/Er doped silicate fibres with Yb co-doping," *Opt. Mater. Express*, vol. 5, no. 10, pp. 2096-2105, Sep. 2015.

Ying Wan is currently working toward the Ph.D. degree in information and communication engineering at Shanghai University, Shanghai, China. Her current research interests include design and fabrication of crystal-derived silica fiber as well as the performance of single-frequency fiber lasers.

Jianxiang Wen received the Ph.D. degree in information and communication engineering from Shanghai University, Shanghai, China and the University of New South Wales, Sydney, Australia. He is currently working as a Professor with the Shanghai Key Lab of Specialty Fiber Optics and Optical Access Network and the School of Communication and Information Engineering of Shanghai University. His major research interests are special optical fiber structures, new optical fiber characteristics, and application research of optical fiber sensing and devices.

Fufei Pang received the Ph.D. degree in optical engineering from Shanghai Institute of Optics and Fine Mechanics of Chinese Academy of Sciences, Shanghai China in 2006. He is currently a Professor of Shanghai University, Shanghai, China. From 2010 to 2011, he was with University of New South Wales, Australia, as a visiting scholar. He is author or co-author of over 100 papers in journals and conference papers, and authored 10 patents. His current research interests include special optical fibers, optical fiber sensors and optical waveguides for optical interconnect.

Tingyun Wang was born in Hebei, China, in 1963. He received the Ph.D. degree in test and measurement technology and instrumentation from the Harbin Institute of Technology, Harbin, in 1998. Now he is the director of Shanghai Key Lab. of Specialty Fiber Optics and Optical Access Network and the dean of School of Communication and Information Engineering of Shanghai University. His major research interests are special fiber optics fabrication, optical interconnection, and fiber optic sensors.